В даному дослідженні проводиться порівняння характеристик циліндричної мезомасштабної камери згоряння з двома плоскими мезомасштабними камерами згоряння, включаючи форму фронту полум'я, температуру осі камери згоряння і стінки камери згоряння, а також межу займистості. Використовувана камера згоряння має кільцевий, квадратний і прямокутний перетин. Всі три камери згоряння мають однакову площу поперечного перерізу і об'єм. Використовуваний стабілізатор полум'я являє собою подвійну вузьку щілину. В якості палива використовується зріджений нафтовий газ з окислювачем на основі чистого кисню. Результати експерименту показали, що циліндрична камера згоряння утворює більш рівномірну форму полум'я, яке заповнює камеру згоряння, і немає чіткого поділу між сторонами полум'я по обидва боки вузької щілини. Високе відношення вхідної і середньої швидкостей призводить до великого позитивного градієнту тиску, який створює вихор і рециркуляцію за стабілізатором полум'я, що дозволяє суміші довше перебувати в камері згоряння (тривалий час перебування). Форма фронту полум'я впливає на температуру осі камери згоряння. Форма фронту полум'я, яке заповнює всю камеру згоряння, має більш високу температуру полум'я, ніж окрема форма фронту полум'я. Кільцева камера згоряння має найвищу середню температуру осі, але найнижчу температуру стінки камери згоряння. Це показує, що кільцева камера згоряння має найменші втрати тепла від полум'я до стінки камери згоряння. Крім того, кільцева мезомасштабна камера згоряння має найбільш широку карту стійкості. При такому ж обсязі кільцева камера згоряння має більш низьке відношення площі поверхні до об'єму, тому тепловтрати також є низькими. Площа мертвої зони також стає більш вузькою, тільки при низькій швидкості реакції. Прямокутні камери згоряння мають найбільше відношення площі поверхні до об'єму, тому втрати також є найбільшими. Незважаючи на найвужчі межі займистості, прямокутні камери згоряння мають найвищі середні температури стінок

Ключові слова: циліндрична мезомасштабна камера згоряння, плоска мезомасштабна камера згоряння, подвійна вузька щілина, відношення вхідної та середньої швидкостей

UDC 532
DOI: 10.15587/1729-4061.2020.198570

PERFORMANCE OF CYLINDRICAL AND PLANAR MESO-SCALE COMBUSTOR WITH DOUBLE NARROW SLIT FLAME HOLDER FOR MICROPOWER GENERATOR

Satworo Adiwidodo
Doctoral Student*
Lecturer
Department of Mechanical Engineering
State Polytechnic of Malang
Jl. Soekarno-Hatta, 9, Malang, Indonesia, 65141
E-mail: satworo.adiwidodo@polinema.ac.id
I. N. G. Wardana
PhD, Professor*
E-mail: wardana@ub.ac.id
Lilis Yuliati
Doctor of Mechanical Engineering,
Assistant Professor*
E-mail: lilis_y@ub.ac.id
Mega Nur Sasongko
Doctor of Mechanical Engineering,
Assistant Professor*
E-mail: megasasongko @ub.ac.id
*Department of Mechanical Engineering
Brawijaya University
Jl. Mayjend Haryono, 167, Malang, Indonesia, 65145

Received date 15.02.2020
Accepted date 15.04.2020
Published date 30.04.2020

1. Introduction

In these two decades, there has been an extraordinary increase in the request for products in a portable form. One of them is the energy source. There have been many studies on energy sources in portable form, among other fuel cells [1, 2], microbattery [3], etc. One of the important things in creating a portable energy source is power density. So far, the highest energy density that we know is nuclear, [4], the next one is hydrogen and then hydrocarbon fuel. People prefer the combustion of hydrocarbon over nuclear for portable energy sources because the handling and safety are more secure. The high energy density of hydrocarbon fuels creates great opportunities for developing portable combustion-based power generation systems [5].

The large energy density of the fuel can be put to good use if the energy converter has high efficiency. The converter for portable combustion-based energy sources in question is a combustor and Thermal Photo Voltaic (TPV) or Thermal Electric (TE). As a photon or thermal provider, the role of the combustor is very important. For portable energy sources, the combustor used has a micro or mesoscale size. Unlike conventional combustors, microscale or mesoscale combustors have a very small size, causing many problems.

The problem that arises in the microscale or mesoscale combustor is the smaller size of the combustion chamber, increase in the surface area to volume ratio (ψ) that causes high heat loss on the flame thus it experiences quenching. The small size also makes fuel residence time low, thus many fuels do not burn completely [6].

For portable energy sources, the combustor flame must be stable and provide a uniform temperature distribution on the wall. Therefore, this study is devoted to reaching a stable flame and provide a uniform temperature distribution on the combustor wall by varying combustor cross-section geometry and using a double narrow slit flame holder. Stable flame and uniform wall temperature are a very important factor for the micropower generator (MPG) in a very broad application. This paper provides a better understanding of the effect of the entrance velocity to the average velocity ratio that determines the flame shape, flow pattern and vortex formation related to heat loss and flame stabilization, also temperature distribution on the combustor wall.

2. Literature review and problem statement

The high energy density of hydrocarbon combustion has attracted many researchers to explore micro/mesoscale combustion devices as a source of energy in micro rotary engines or gas turbines, thermophotovoltaic, or thermoelectric systems or better known as micropower plants [7]. To be able to produce high energy, the micro/mesoscale combustor must be able to produce a stable flame. The small size of the micro/mesoscale combustor is a big problem in terms of flame stability. It is understood that the problem of stabilizing the flame on the micro/mesoscale combustor first is due to the amount of heat loss on the wall due to the large surface area to volume ratio thus the flame experiences a quenching. The small size of the combustor also results in the short residence time of the fuel in the combustion chamber, thus the fuel and oxidizer do not have enough time to react perfectly, especially at high fuel rates. Even though high fuel rates are needed to produce large amounts of energy.

One way to reduce heat loss is by recirculating heat in the combustor as in the swiss roll combustor model [8]. Another method for reducing heat loss in micro or mesoscale combustors with external heating is to improve flame stability [9]. Several studies have been conducted to overcome the short residence time, including accelerating the combustion reaction to produce a stable flame using a catalyst [10–12]. Premixed catalytic combustion of methane-air in rectangular microchannels has been studied experimentally. The test results showed that the flammability limit increases significantly when platinum is added to the microchannel. The addition of catalysts in the channel not only provides a uniform temperature distribution in the outer walls of the channel but also increases methane conversion [10]. Problems related to the low-temperature catalytic oxidation of synthesis gas at high pressure under lean-burn conditions are discussed in other studies. The study was carried out in numerical simulations to explore the mechanism responsible for the interaction between carbon monoxide and hydrogen during the combined oxidation process [11]. It appears that there is a strong interaction between carbon monoxide and hydrogen during the combined oxidation process. An experimental study of electro-spraying and ethanol combustion on a mesoscale conducted on a combustor with a catalyst showed ethanol combustion efficiency could be increased by 4.5 %, which proves that platinum catalysts can accelerate ethanol decomposition [12].

Other studies to accelerate the rate of combustion reactions use pure oxygen as oxidizers [13–16]. Flame methane-oxygen diffusion without a catalytic microburner shows the number of flame cells observed depends on the velocity of the inlet gas and the initial mixture [13]. In the combustion of methane-oxygen, at an equivalence ratio of less than one, CH_4 is not fully oxidized and large amounts of H_2 and CO gas are produced, this reduces combustion heat. If the equivalence ratio is slightly greater than one, CH_4 is fully oxidized to CO_2 gas and water vapor, and the reaction produces maximum combustion heat [14]. Other studies using methane-oxygen with nitrogen dilution concluded that by increasing the velocity of the inlet mixture, the equivalence ratio must be reduced from the rich mixture to stoichiometric values to create a stable flame in the mesoscale combustor [15]. Non-adiabatic research of premixed methane-oxygen at the combustor d=1 mm and d=2 mm shows that reducing the diameter in the reactor can significantly influence the operational regime of flame and propagation velocity in the reactor in terms of suppressing hydrodynamic instability [16].

Short residence time can also be overcome by adding a bluff body. The effects of bluff body dimensions on micro-planar have been investigated by numerical simulation. They revealed that the recirculation zone produced a group of radicals with a low velocity that dominated flame stabilization [17]. The shape of the combustion chamber with cavities is also used to prolong the reactant residence time. From experimental studies, it is shown that cavities have a strong ability to expand the operational range of velocity entrance and numerical simulations show that low-velocity zones occur in the cavity [18]. The synergistic effect of bluff-body and cavity is that the critical velocity increases and the appearance of the recirculation zone increases the stability of the flame [19].

The role of the flame holder is also very important in the process of flame stabilization. Several types of flame holders have been tried, including porous media [20], wire mesh [21], backward-facing step [22], and slit [23–25]. Turbulent intensity on Micro-Combustor with Slits on both sides of the Bluff Body (MCSB) is greater thus it prolongs residence time and increases combustion efficiency and velocity extinction limit [24]. The use of a double flame slit flame holder has successfully expanded the stability map and shifted the equivalence ratio to the lean mixture region [25].

Combustion in micro/mesoscale combustors with air oxidizing agents has a different characteristic compared to combustion with pure oxygen oxidizing agents. Combustion with pure oxygen produces a very rapid flame propagation rate. To overcome this, the narrow slit flame holder is used to stabilize the flame in a mixture of liquefied petroleum gas (LPG) and oxygen. In preliminary research, it is known that in combustors with rectangular slots in different aspect ratios, various flame modes arise [25]. The difference in flame modes is related to the heat loss in the combustor related to the difference in the aspect ratio of the combustor cross-section. In that study, the same narrow slit flame holder was used, resulting in differences in the reactant entrance area when entering the combustor. For the same fuel discharge, it will produce a different entrance velocity. This will certainly have a significant effect on the combustion process and flame stabilization in the mesoscale combustor. This has not been discussed in previous studies. This research was conducted on 3 types of combustors (circular, square, rectangle), to know the effect of the entrance area on the narrow slit flame holder on the combustion characteristics in the mesoscale combustor, related to the ratio between the entrance velocity and average velocity, flow patterns and vortex formation near the flame holder with a double narrow slit and heat loss mechanism from the flame to the combustor wall.

3. The aim and objectives of the study

This research aims to study the effect of the entrance to average velocity ratio as a result of implementing the use of the same narrow slit flame holder in different combustion geometries, which affects the stability of the flame and the temperature that can be achieved, and its uniformity in the combustor wall.

To achieve this aim, the following objectives are accomplished:

– to study the influence of the combustor cross-section geometry related to the entrance area and the ratio of entrance velocity to average velocity on the flame visualization inside the mesoscale combustor;

– to study the influence of flame visualization on flame temperature and combustor walls and their relationship to heat loss from a flame to combustor walls;

– to study the influence of the entrance to average velocity ratio on flow patterns and vortex formation and its relationship to flammability limits.

4. Materials and methods of experimental research

3 types of combustors with different forms of cross-sections, namely cylindrical, square and rectangular, are used (Fig. 1). The dimensions of the combustor are shown in Table 1. Since this study uses two types of combustors, circular and non-circular, then the geometry parameter is represented by the hydraulic diameter (D_h). Hydraulic diameter is the diameter representation for non-circular geometry. In a circular one, the hydraulic is the same as the normal diameter. The cross-section area of the combustor (A_c) is the same for each type that is 6 mm^2. The shape of the flame holder is a cylinder of 8 mm in diameter and 4 mm thick with 2 narrow slits each measuring of 0.2×3.8 mm^2 as shown in Fig. 2. The combustor and flame holder were made of copper.

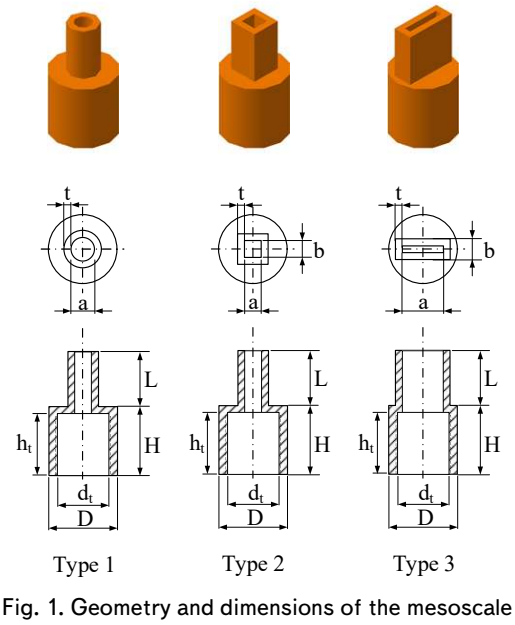

Fig. 1. Geometry and dimensions of the mesoscale combustor

Table 1

Combustor geometry specifications

Combustor type	a (mm)	b (mm)	t (mm)	L (mm)	H (mm)	h_t (mm)	D (mm)	d_t (mm)	D_h (mm)	A_c (mm^2)
1	2.76	–	1	8	10	9	10	8	2.76	6
2	2.45	2.45	1	8	10	9	10	8	2.45	6
3	1	6	1	8	10	9	10	8	1.71	6

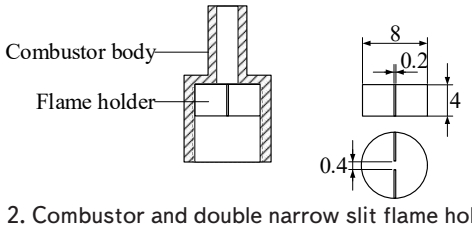

Fig. 2. Combustor and double narrow slit flame holder geometry and dimensions

The LPG was burned in premixed with pure oxygen (99.99 %), therefore various types of stability modes in the mesoscale combustion chamber can be observed. The LPG composition is shown in Table 2. The composition of LPG consists of a mixture of propane (48.86 %), N-butane (31.64 %), iso-butane (18.91 %), and the rest are other gases with very small amounts.

Table 2

LPG composition

Composition	% Volume
Propane	48.86
N-butane	31.64
Iso-butane	18.91
Ethane	0.42
Neo-pentane	0.10
Iso-pentane	0.07

LPG and oxygen flow rates were measured with a Kofloc flow meter with a measurement range of 2–20 mL/min for LPG fuel and 50–500 mL/min for oxygen. Fuel and oxygen were mixed in a mixer before being burned in the combustion chamber. Premixed combustion was done in a horizontal combustor position. The schematic of the test section for this study is shown in Fig. 3.

Data taken from this experiment included visual data, which include visualization of the flame front view and visualization of the combustor wall. Visualization of the flame and combustor wall was performed using a Canon EOS 60 D camera. The next data was temperature. Temperature measurements were made on the wall and combustor axis. Type R thermocouples (Pt-13 % Rh/Pt) were used to measure temperatures on the combustor axis while type K (Nickel-Chromium) thermocouples were used to measure the temperature of the combustor wall. The thermocouple was connected to the NI USB-TC01 data logger as data acquisition. The temperature was measured at a distance of P_1=1 mm, P_2=5 mm, and P_3=9 mm from the entrance as shown in Fig. 3. The zero points were measured from the surface of the flame holder. The $U_{average}$ is the reactant flow rates measured in the combustor cross-section.

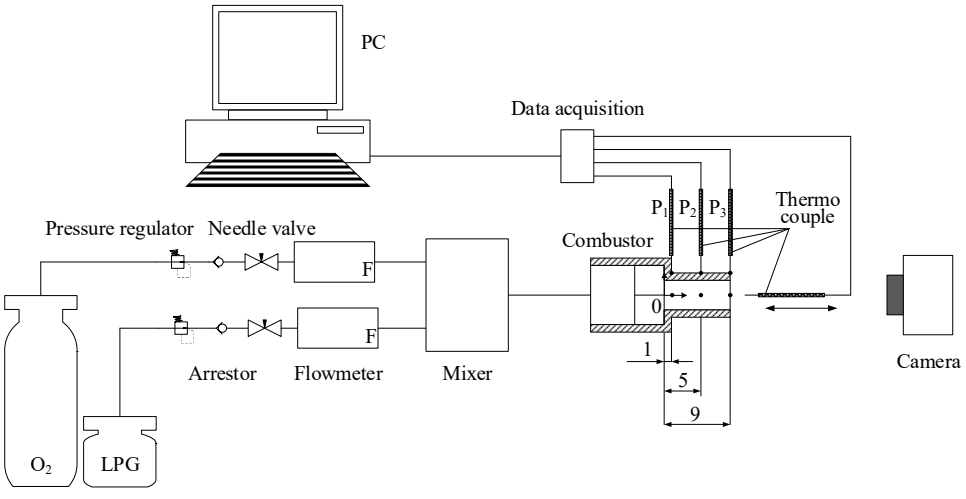

Fig. 3. Schematic of the test section and points of temperature measurement

Temperature measurements were carried out at the reactant flow rates $U_{average}$=50, 75, and 100 cm/s at the equivalence ratio of ϕ=0.3, 0.8, 1, and 1.2. Measurements on the combustor axis were performed to measure the flame temperature and its effect on the flammability limit. The wall temperature measurement was used to compare the uniformity of the combustor wall temperature. Retrieval of temperature data was done after getting a map of flame stability. The flame stability limit data were obtained by maintaining a constant mass flow rate of oxygen while varying the mass flow rate of the fuel and vice versa. The amount of data recorded for each combustor was more than 3,000 data. Data points inside the stability area were removed, leaving the outermost point as the boundary of each region. The flame was considered stable when it was able to survive to burn in steady conditions for 10 minutes.

5. Result performance of cylindrical and planar mesoscale combustor with double narrow slit flame holder for micropower generator

5. 1. Effect of geometrical cross-section on flame front color and shape and wall illumination

Fig. 4 shows the visualization of the flame seen from the front in the combustor mesoscale at reactant rates $U_{average}$=50, 75 and 100 cm/s. Equivalence ratios vary in the range of ϕ=0.3–1.2. All forms of cross-section showed the same tendency, which is, the shape of the flame increasingly fills the entire combustor cross-section with the increase in the average reactant velocity. The color of the flame that was originally dark blue leads to bright light blue. Likewise, the increase in equivalence ratios caused more diffuse and bright blue flames.

The shape of the flame was also strongly influenced by the flame holder in the form of a double narrow slit. In circular combustors, the flame shape similar to the shape of the holder slit occurred only at low equivalence ratios. In the square combustor, the flame shape similar to the holder slit occurred not only at low equivalence ratios but also at low velocities. The flame shape similar to the slit holder in the rectangular combustor occurs in all combinations of equivalence ratio and reactant rate. The flame in the circular combustor appeared separated at ϕ=0.3, at a greater equivalence ratio no flame separation occurred. Square combustor produces a solid flame at a high equivalence ratio and average reactant velocity. While the rectangular combustor at all the equivalence ratios and average velocity produced a flame that appeared to be separated.

Fig. 5 shows the illumination of the combustor wall. Circular combustor wall smoldering at ϕ=0.8–1.2, at a reactant velocity above 75 cm/s. Square combustor had a narrower wall illumination, i. e. for ϕ=0.8–1.2 at a reactant velocity of 100 cm/s. The rectangular shape had the broadest smolder area, namely at ϕ=0.8–1.2 and reactant rates above 50 cm/s. The higher the equivalence ratio, the more illumine the wall, as well as an increase in the reactant rate. Rectangular combustor at ϕ=1.2 and the reactant velocity of 100 cm/s had the highest combustor wall illumination.

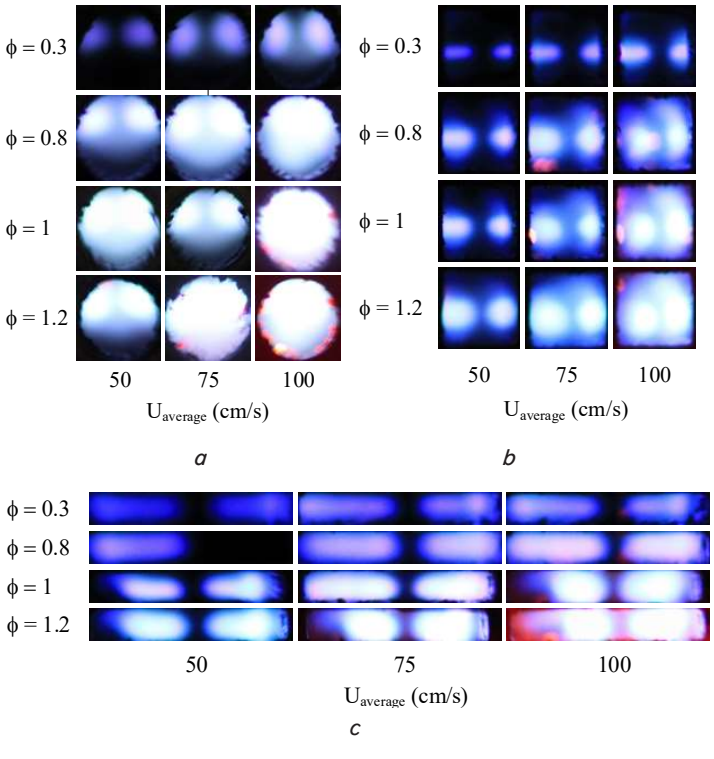

Fig. 4. Flame front at various $U_{average}$ and equivalence ratio (ϕ): *a* – circular combustor; *b* – square combustor; *c* – rectangular combustor

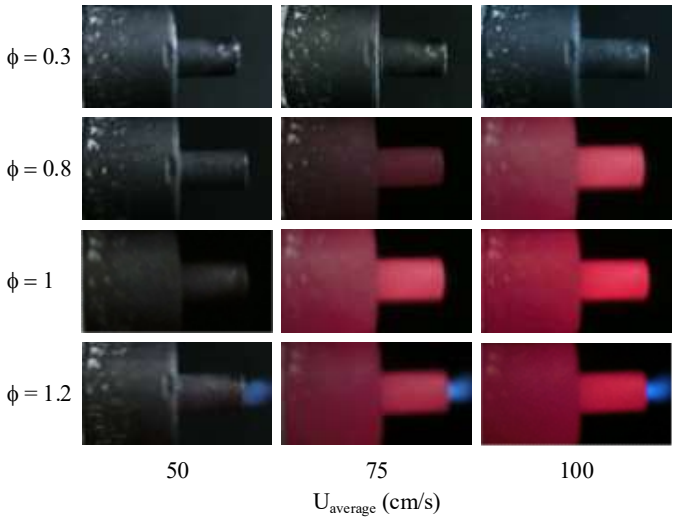

a

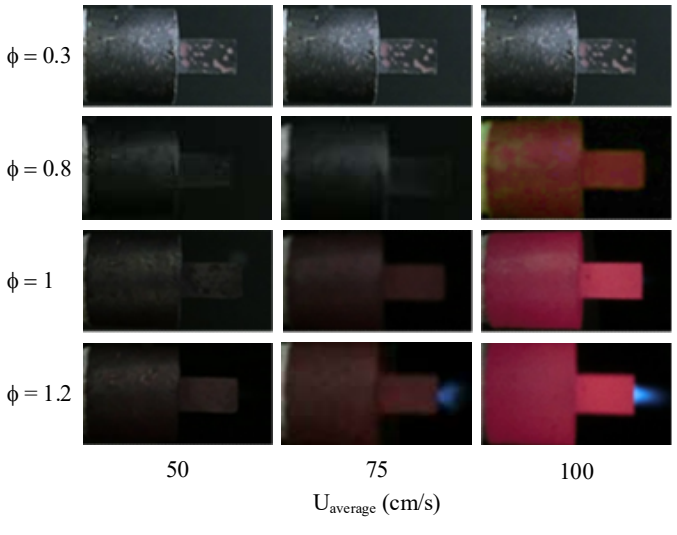

b

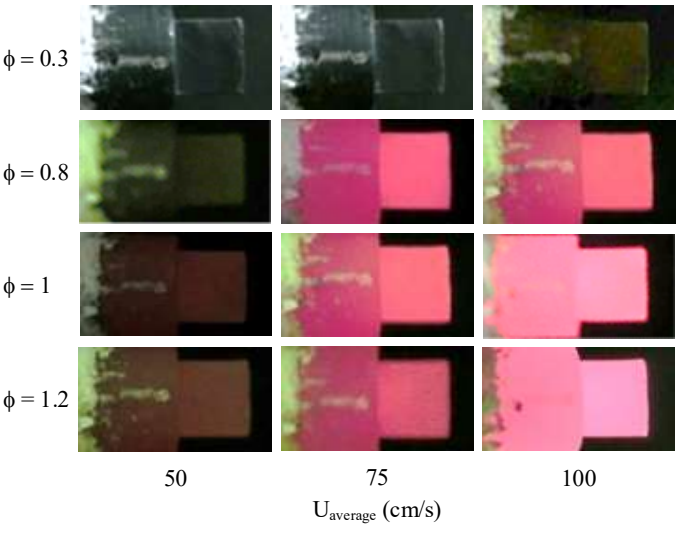

c

Fig. 5. Combustor wall illumination at various $U_{average}$ and equivalence ratio (ϕ): *a* —circular combustor; *b* — square combustor; *c* — rectangular combustor

The higher the temperature in the combustor wall, the higher the combustor wall illumination. The highest combustor wall illumination is achieved by a rectangular combustor (Fig. 5). This shows that the rectangular combustor's heat loss is the highest. The heat generated by the flame is released to heat the combustor wall. Wall temperatures can reach high and uniform temperatures, which are needed for applications in micropower generators. However, the amount of heat loss will affect the stability and flammability limit that can be achieved.

5. 2. Effect of geometrical cross-section on the combustor axis and wall temperature

Fig. 6. shows the average temperature along the combustor axis with various forms of combustor cross-section at a reactant rate $U_{average}$=100 cm/s. There was an increase in average temperature as the ratio increased to a value of about 1, then there was a downward trend. The highest average temperature was achieved by a circular combustor. While the lowest average axis temperature was achieved by a rectangular combustor.

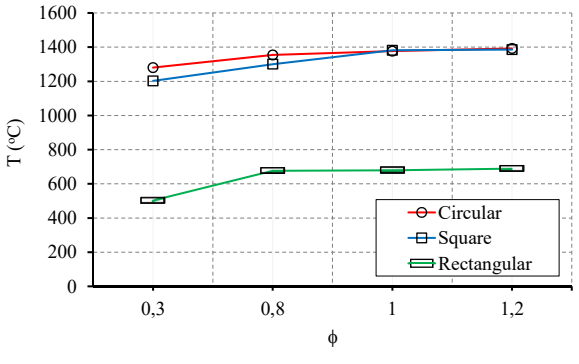

Fig. 6. Average combustor axis temperature at $U_{average}$=100 cm/s

The average temperature of the wall is shown in Fig. 7. As the temperature distribution on the combustor axis, the average temperature of the wall increased sharply at ϕ=0.3 until ϕ=1 then there was a tendency to decrease with the addition of the equivalence ratio, even from the measurement on ϕ=1.2 produced the highest temperature. The highest average wall temperature was produced by a rectangular combustor, and the lowest average was a circular combustor.

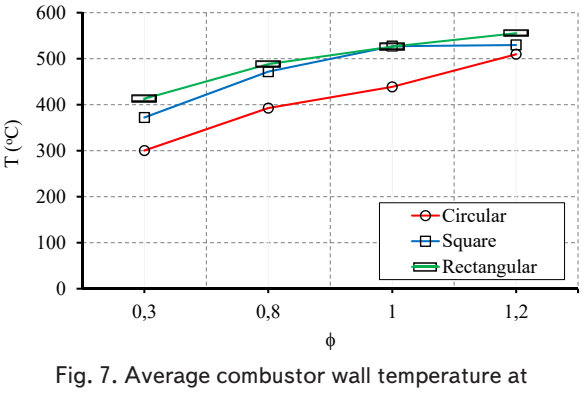

Fig. 7. Average combustor wall temperature at $U_{average}$=100 cm/s

The average temperature on the rectangular combustor wall is the highest at all equivalence ratios. Square wall temperature ranks second to the highest and the lowest is the circular combustor. This is the opposite of the temperature measured in the combustor axis. High temperatures in the axis do not always produce high temperatures in the walls. Heat loss is very influential on the temperature achieved by the combustor wall.

5. 3. Effect of geometrical cross-section on flammability limit

Different forms of combustor cross-section produce different flammability limits as shown in Fig. 8–10. As with preliminary work, there were six observed flame modes, which are stable without noise, stable with noise, transition zones, dead zones, pseudo-stable, and blow-off limits. Stable without noise is when the flame can light up 10 minutes without sound. When the flame can ignite stable for 10 minutes but makes a sound then it goes into the stable with noise mode. The transition zone is an area where the flame conditions sometimes appear sound, then silence alternately and can last for 10 minutes. The dead zone is a very reactive area where a flame cannot be stabilized and causes an explosion. Pseudo stable is an area where a flame can be maintained in less than 10 minutes. The blow-off limit is the limit where if the ratio equivalence shifts to the left of the line, the flame will be blown and extinguished.

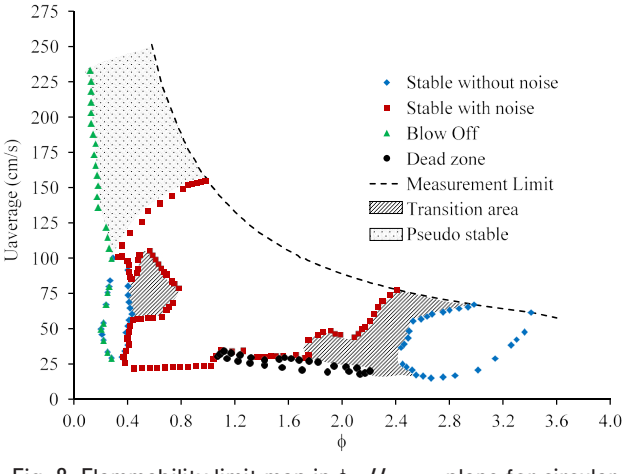

Fig. 8. Flammability limit map in $\phi-U_{average}$ plane for circular combustor

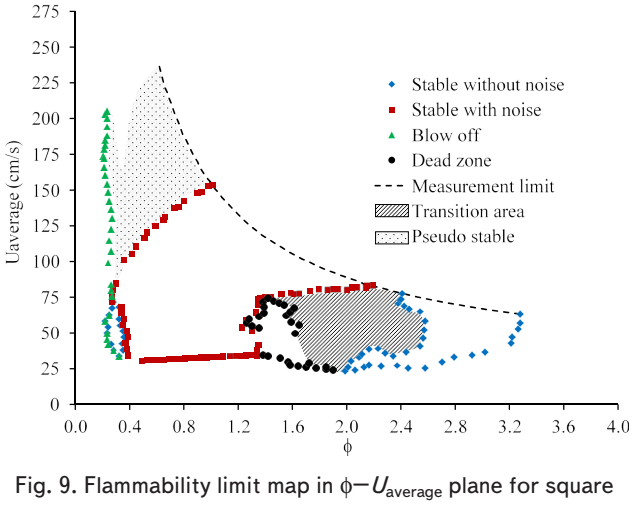

Fig. 9. Flammability limit map in $\phi-U_{average}$ plane for square combustor

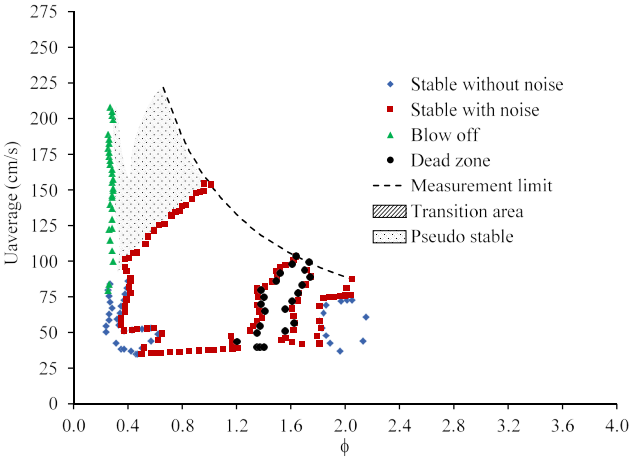

Fig. 10. Flammability limit map in $\phi-U_{average}$ plane for rectangle combustor

Stable areas without noise in all forms of combustor cross-section occurred at the equivalence ratio of the very lean mixture and very rich mixture and low reactant rates. Circular combustors had the broadest stable without noise areas in both lean mixture and rich mixture (Fig. 8). Lean mixture regions in the equivalence ratio range were almost the same for all combustor forms. As for rich mixture, the maximum equivalence ratio was different, for circular combustors at φ=3.4, square combustor at φ=3.3, and the lowest were rectangular at φ=2.2. Stable areas with noise were located in the area of the equivalence ratio range above φ=0.3. The maximum limit of equivalence ratios in this area was different in each combustor type. At an equivalence ratio of about 1 (stoichiometric), the noise intensity was very high and decreased in the rich mixture and lean mixture. Stable with noise is the widest achieved by circular combustors and narrowest by rectangular combustors. A transition zone is a zone between stable and silent regions. The circular combustor transition zone was in a lean mixture at φ=0.4–0.8, and a rich mixture φ=1.8–3. The circular combustor transition zone is the most extensive. In square combustors, the transition zone only occurred in a rich mixture (Fig. 9). In lean mixture there was no transition zone, the boundary was stable without sound and stable with very clear sound. The transition zone in the combustor square occurred in the equivalence ratio range of φ=1.4–2.6. In the rectangular combustor, there was no visible transition zone in both lean mixture and rich mixture. The dead zone is an area where a flame cannot be ignited at all, the flame immediately experiences flashback and goes out. Dead zones are different from the usual flashback phenomena because they not only occur at low reactant rates but also occur at high reactant rates and are accompanied by explosions. The dead zone in a circular combustor occurred in a very narrow area at low velocity at the bottom of the flammability limit map. The square combustor has a larger dead zone area with a higher reactant velocity. The rectangular combustor has the largest area and highest reactant velocity. All dead zones occurred at equivalence ratios above 1. Pseudo-stable is a stable area with noise but unable to maintain a flame for 10 minutes. The largest pseudo stable region occurred in the circular combustor and the smallest in the rectangular combustor. The blow off line showed that when the reactant mixture was made leaner, the flame will be released from the flame holder and blown out. The blow-off limit was on the three different

combustors. Circular combustor blow off limit at the lowest equivalence ratio, square blow off limit at a higher, whereas rectangular at the highest.

6. Discussion of the results of studying the performance of cylindrical and planar mesoscale combustor with double narrow slit flame holder for micropower generator

The same flame holder, when applied to different combustor cross-section geometries, will produce different entrance areas (shaded) as shown in Fig. 11. Consequently, for the average velocity in the same combustion chamber, there was a difference in entrance velocity.

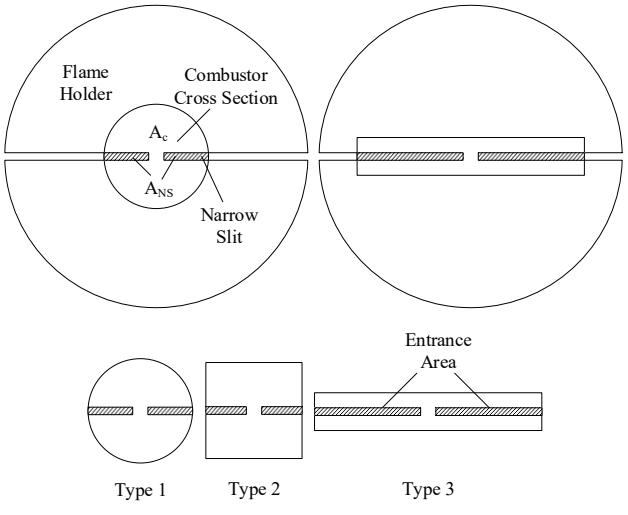

Fig. 11. Geometry of the flame holder to the combustor cross-section

The velocity ratio can be calculated with continuity. When incompressible flow was assumed, the ratio of the entrance and the average velocity in the combustor (U_R) can be calculated by the following formula:

$$\dot{m}_1 = \dot{m}_2, \tag{1}$$

$$\rho_1 A_1 V_1 = \rho_2 A_2 V_2, \tag{2}$$

$$U_R = \frac{U_{\text{entrance}}}{U_{\text{average}}}, \tag{3}$$

$$U_R = \frac{U_{entrance}}{U_{average}} = \frac{V_1}{V_2} = \frac{A_2}{A_1} = \frac{A_C}{A_{NS}}, \tag{4}$$

where V_1 is the velocity at the entrance, i.e. in a narrow slit area, and V_2 is the average velocity in the combustor. A_1 is the area at the entrance or narrow slit (A_{NS}), and A_2 is the area of the combustor cross-section (A_c).

The results of calculations of U_R are presented in Table 3. It can be seen that the square combustor had the highest entrance to the average velocity ratio, then the value that approached the circular combustor and the lowest was the rectangular combustor.

When we compare the flame shape to the front view (Fig. 4), it can be seen that when U_R was high, the flame shape to the front looked solid. The flame can fill the entire combustor. The large velocity difference between the entrance area and inside the combustor created a high-pressure gradient. Low static pressure at the entrance will meet with high static pressure at the combustor. Reactants can be delivered to the combustor only because of the kinetic energy of the flow. This caused the fuel to be squeezed from both sides and made the fuel more evenly fill the entire room in the combustor which created a full flame shape. Although the square shape had the largest U_R, the flame shape looked more full on circular combustors with U_R slightly below it. The surface area inside the combustor (A_S) of each geometry can be calculated. For the known combustor volume (Vol), the surface area to volume ratio (ψ) will be obtained as shown in Table 4. From Table 4 it appears that the square combustor had a surface area to volume ratio greater than the circular type which caused a large heat loss thus the flame will quench when close to the wall.

Table 3

Entrance to average velocity ratios for each combustor type

Combustor type	A_c (mm^2)	A_{NS} (mm^2)	U_R
1	6	0.4716	12.72
2	6	0.41	14.63
3	6	1.12	5.36

Table 4

Surface area to volume ratio

Combustor type	A_s (mm^2)	Vol (mm^3)	ψ
1	83.526	54	1.56
2	93.7925	54	1.74
3	130.88	54	2.44

From Fig. 4 it can also be seen that the greater the equivalence ratio, the brighter the color. An increase in the equivalence ratio means that more reactants are burned. This caused an increase in flame temperature (Fig. 6). This temperature rise caused the flame color to look brighter. The greater equality ratio also made the flame shape wider. The same effect was produced when the average reactant velocity increased.

The flame was solid and filled the entire combustion chamber, resulting in high temperatures. This was evidenced by the high combustor axis temperature achieved by the circular shape (Fig. 6). The circular cross-section shape reached the highest axis temperature at all equivalence ratios compared to the other two combustors. In the measurement of the wall temperature, the circular combustor showed the lowest average results (Fig. 7), this is following the fact that at the same combustor volume, the circular combustor had the lowest surface area to volume ratio which created heat loss in small walls. These two things made the flammability limit in the circular combustor the widest (Fig. 8). The highest wall temperature was achieved by the rectangular combustor (Fig. 7). This fact shows that the heat transfer from the flame to the combustion chamber wall is the largest in the rectangular combustor so the highest combustor wall illumination is achieved (Fig. 5), although the heat produced by the combustion process in the combustion chamber is the smallest. That is the reason why this combustor had the narrowest flammability limit (Fig. 10).

The burning velocity of the circular combustor was definitely the highest. The burning velocity was affected by the flame temperature. While the flame temperature was affected by how much heat was generated and heat loss, and heat loss is affected by the interaction of flame and walls. Rectangular combustors had the smallest hydraulic diameter. That made the distance of flame to the wall closest to the other 2 types of combustor experienced more heat being absorbed by the combustor wall. The mechanism of heat loss in the combustor wall is shown in Fig. 12.

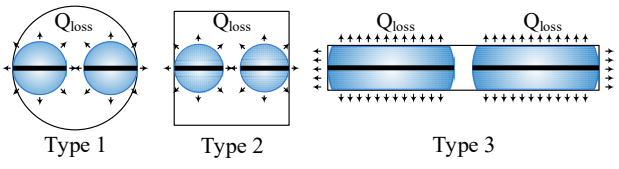

Fig. 12. Heat loss on combustor wall

The flame stabilization process is also determined by how the flow pattern is formed in the area near the flame holder. The higher U_R generates stronger vortices and causes recirculation flow behind the flame holder which helps stabilize the flame shown in Fig. 13. The formation of the recirculation flow and the vortex behind the flame holder was strengthened by the presence of a bluff body. The flammability limit map in Fig. 8–10 shows the circular combustor had the most extensive area in almost all modes of stability, except for areas in the dead zone. The smallest circular dead zone area occurred at low rates in the range ϕ=0.9–2.2. The reduction of the dead zone results from reduced heat loss in the circular combustor (ϕ=1.61).

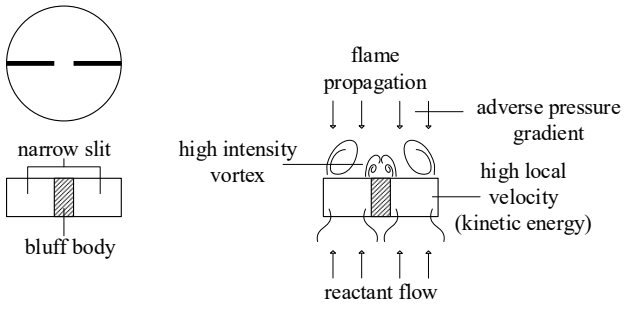

Fig. 13. Stabilizing mechanism and vortex formation on the flame holder

This research produced something important, including reducing the dead zone by reducing the surface area to volume ratio of the combustor by making a circular combustor shape. However, for practical needs, both thermoelectric and thermophotovoltaic, high and uniform wall temperatures are required as in the rectangular combustor. The challenge of future research is how to produce a combustor design that can reduce dead zones, but has a high and uniform wall temperature. Noise reduction is also a very interesting topic to study.

7. Conclusions

1. The ratio of the entrance velocity to average velocity has been shown to influence the shape of the flame. The flame shape of the circular combustor which has a high U_R (12.72) is more widespread in the entire combustor field. The large velocity difference between the entrance area and the combustion chamber causes a large adverse pressure gradient that makes the fuel last longer in the combustion chamber. The flame shape on the rectangular combustor (U_R=5.36) clearly shows the flame separation on both sides of the slit.

2. The shape of the flame seen from the front affects the temperature of the flame. The solid flame shape that fills the entire combustion chamber has a higher flame temperature than the separate flame shape. The highest flame temperature is achieved by the circular combustor and the lowest is the rectangular combustor. The shape of the combustor cross-section affects the wall temperature concerning the surface area to volume ratio (ψ) that is different. Rectangular combustors have the largest surface area to volume ratio, thus the losses are also the biggest which causes the highest wall temperatures.

3. The large entrance to the average velocity ratio, in addition to causing a large adverse pressure gradient, also makes the fuel last longer in the combustion chamber and also creates a recirculation flow pattern that helps stabilize the flame near the flame holder. The formation of vortices is reinforced by the shape of the bluff body in the center of the flame holder. Flame holders with this unique shape also contribute to reactant heating before entering the combustion chamber. We recommend this flame holder, especially for combustors that use oxygen because it can delay flashback. The widest flammability limit is achieved by the circular combustor, and the narrowest is the rectangular combustor. Despite the narrowest flammability limits, rectangular combustors have the highest average wall temperatures.

References

1. Sharaf, O. Z., Orhan, M. F. (2014). An overview of fuel cell technology: Fundamentals and applications. Renewable and Sustainable Energy Reviews, 32, 810–853. doi: https://doi.org/10.1016/j.rser.2014.01.012
2. Staffell, I., Scamman, D., Velazquez Abad, A., Balcombe, P., Dodds, P. E., Ekins, P. et. al. (2019). The role of hydrogen and fuel cells in the global energy system. Energy & Environmental Science, 12 (2), 463–491. doi: https://doi.org/10.1039/c8ee01157e
3. Oudenhoven, J. F. M., Vullers, R. J. M., Schaijk, R. (2012). A review of the present situation and future developments of micro-batteries for wireless autonomous sensor systems. International Journal of Energy Research, 36 (12), 1139–1150. doi: https://doi.org/10.1002/er.2949
4. Chou, S. K., Yang, W. M., Chua, K. J., Li, J., Zhang, K. L. (2011). Development of micro power generators – A review. Applied Energy, 88 (1), 1–16. doi: https://doi.org/10.1016/j.apenergy.2010.07.010
5. Ju, Y., Maruta, K. (2011). Microscale combustion: Technology development and fundamental research. Progress in Energy and Combustion Science, 37 (6), 669–715. doi: https://doi.org/10.1016/j.pecs.2011.03.001

6. Kaisare, N. S., Vlachos, D. G. (2012). A review on microcombustion: Fundamentals, devices and applications. Progress in Energy and Combustion Science, 38 (3), 321–359. doi: https://doi.org/10.1016/j.pecs.2012.01.001
7. Nakamura, Y., Gao, J., Matsuoka, T. (2017). Progress in small-scale combustion. Journal of Thermal Science and Technology, 12 (1), JTST0001–JTST0001. doi: https://doi.org/10.1299/jtst.2017jtst0001
8. Zhong, B.-J., Wang, J.-H. (2010). Experimental study on premixed CH4/air mixture combustion in micro Swiss-roll combustors. Combustion and Flame, 157 (12), 2222–2229. doi: https://doi.org/10.1016/j.combustflame.2010.07.014
9. Zhou, J., Wang, Y., Yang, W., Liu, J., Wang, Z., Cen, K. (2009). Improvement of micro-combustion stability through electrical heating. Applied Thermal Engineering, 29 (11-12), 2373–2378. doi: https://doi.org/10.1016/j.applthermaleng.2008.12.005
10. Pan, J., Zhang, R., Lu, Q., Zha, Z., Bani, S. (2017). Experimental study on premixed methane-air catalytic combustion in rectangular micro channel. Applied Thermal Engineering, 117, 1–7. doi: https://doi.org/10.1016/j.applthermaleng.2017.02.008
11. Chen, J., Yan, L., Song, W., Xu, D. (2018). Catalytic Oxidation of Synthesis Gas on Platinum at Low Temperatures for Power Generation Applications. Energies, 11 (6), 1575. doi: https://doi.org/10.3390/en11061575
12. Gan, Y., Tong, Y., Jiang, Z., Chen, X., Li, H., Jiang, X. (2018). Electro-spraying and catalytic combustion characteristics of ethanol in meso-scale combustors with steel and platinum meshes. Energy Conversion and Management, 164, 410–416. doi: https://doi.org/10.1016/j.enconman.2018.03.018
13. Miesse, C., Masel, R., Short, M., Shannon, M. (2005). Experimental observations of methane–oxygen diffusion flame structure in a sub-millimetre microburner. Combustion Theory and Modelling, 9 (1), 77–92. doi: https://doi.org/10.1080/13647830500051661
14. Li, J., Zhong, B. (2008). Experimental investigation on heat loss and combustion in methane/oxygen micro-tube combustor. Applied Thermal Engineering, 28 (7), 707–716. doi: https://doi.org/10.1016/j.applthermaleng.2007.06.001
15. Sarrafan Sadeghi, S., Tabejamaat, S., Baigmohammadi, M., Zarvandi, J. (2014). An experimental study of the effects of equivalence ratio, mixture velocity and nitrogen dilution on methane/oxygen pre-mixed flame dynamics in a meso-scale reactor. Energy Conversion and Management, 81, 169–183. doi: https://doi.org/10.1016/j.enconman.2014.02.022
16. Baigmohammadi, M., Tabejamaat, S., Yeganeh, M. (2019). Experimental study of methane-oxygen premixed flame characteristics in non-adiabatic micro-reactors. Chemical Engineering and Processing - Process Intensification, 142, 107590. doi: https://doi.org/10.1016/j.cep.2019.107590
17. Fan, A., Wan, J., Liu, Y., Pi, B., Yao, H., Maruta, K., Liu, W. (2013). The effect of the blockage ratio on the blow-off limit of a hydrogen/air flame in a planar micro-combustor with a bluff body. International Journal of Hydrogen Energy, 38 (26), 11438–11445. doi: https://doi.org/10.1016/j.ijhydene.2013.06.100
18. Wan, J., Fan, A., Liu, Y., Yao, H., Liu, W., Gou, X., Zhao, D. (2015). Experimental investigation and numerical analysis on flame stabilization of CH4/air mixture in a mesoscale channel with wall cavities. Combustion and Flame, 162 (4), 1035–1045. doi: https://doi.org/10.1016/j.combustflame.2014.09.024
19. Zhang, Z., Wu, K., Yao, W., Yuen, R., Wang, J. (2020). Enhancement of combustion performance in a microchannel: Synergistic effects of bluff-body and cavity. Fuel, 265, 116940. doi: https://doi.org/10.1016/j.fuel.2019.116940
20. Chen, X., Li, J., Feng, M., Zhao, D., Shi, B., Wang, N. (2019). Flame stability and combustion characteristics of liquid fuel in a meso-scale burner with porous media. Fuel, 251, 249–259. doi: https://doi.org/10.1016/j.fuel.2019.04.011
21. Yuliati, L. (2014). Flame Stability of Gaseous Fuel Combustion inside Meso-Scale Combustor with Double Wire Mesh. Applied Mechanics and Materials, 664, 231–235. doi: https://doi.org/10.4028/www.scientific.net/amm.664.231
22. Sanata, A., Wardana, I. N. G., Yuliati, L., Sasongko, M. N. (2019). Effect of backward facing step on combustion stability in a constant contact area cylindrical mesoscale combustor. Eastern-European Journal of Enterprise Technologies, 1 (8 (97)), 51–59. doi: https://doi.org/10.15587/1729-4061.2019.149217
23. Adiwidodo, S., Wardana, I. N. G., Yuliati, L., Sasongko, M. N. (2016). Flame Stability Measurement on Rectangular Slot Meso-Scale Combustor. Applied Mechanics and Materials, 836, 271–276. doi: https://doi.org/10.4028/www.scientific.net/amm.836.271
24. Yan, Y., He, Z., Xu, Q., Zhang, L., Li, L., Yang, Z., Ran, J. (2019). Numerical study on premixed hydrogen/air combustion characteristics in micro–combustor with slits on both sides of the bluff body. International Journal of Hydrogen Energy, 44 (3), 1998–2012. doi: https://doi.org/10.1016/j.ijhydene.2018.11.128
25. Adiwidodo, S., Wardana, I. N. G., Yuliati, L., Sasongko, M. N. (2019). Development of planar mesoscale combustor with double narrow slit flame holder and various aspect ratios for micropower generator. Eastern-European Journal of Enterprise Technologies, 1 (8 (97)), 14–23. doi: https://doi.org/10.15587/1729-4061.2019.155663